Monte Carlo Study of Polyelectrolyte Adsorption. Isolated Chains on a Planar Charged Surface

Sagrario Beltrán,† Herbert H. Hooper,‡ Harvey W. Blanch, and John M. Prausnitz*

Chemical Engineering Department and Materials and Chemical Sciences Division, Lawrence Berkeley Laboratory, University of California, 1 Cyclotron Road, Berkeley, California 94720

Received July 3, 1990; Revised Manuscript Received December 17, 1990

ABSTRACT: Monte Carlo simulations are presented for the adsorption of a lattice-model isolated polyelectrolyte on an impenetrable, oppositely charged surface. We consider the effects of chain ionization, chain hydrophobicity, surface charge density, and solution ionic strength on the conformational and interfacial properties of the model system. The overall conformational properties of the model polyelectrolytes in the adsorbed state are similar to those of isolated polyelectrolytes in solution; however, the adsorbed chains are conformationally anisotropic. This anisotropy is described here by calculating the components of the polymer end-to-end distance in directions parallel and orthogonal to the interface. Detailed structural features of the adsorbed chains are described by the distributions of tails, trains, and loops. Tails are favored at low degrees of chain ionization, while trains become more favorable at high degrees of ionization. The number of adsorbed chain segments (e.g., degree of adsorption) increases with the surface charge density and decreases with increasing solution ionic strength; for some conditions, this degree of adsorption is a strong function of solution and surface properties.

I. Introduction

Polyelectrolytes are important for various technical applications, including use as viscosifiers in oil recovery, as flocculants in water treatment, as wet-end additives in the paper-making process, and as erosion preventers in soil conditioning. For many applications, the rheological behavior of these systems is of primary interest. However, in other cases, the interactions of polyelectrolytes with surfaces are of major (or primary) concern.

Theories for describing polyelectrolyte adsorption have typically followed by several years the development of models for adsorption of uncharged polymers. Hesselink presented in 1972[1,2] the first theory for polyelectrolyte adsorption, based on the earlier work of Hoeve[3] for adsorption of *uncharged* flexible polymers; both models require that the segment concentration profile near the surface is known a priori. For uncharged polymers, Roe[4] later developed a multilayer lattice theory in which the segment-density profile near the surface is determined self-consistently. Roe's theory considers only segment-density variations normal to the surface and does not identify specific molecular conformations at the surface. Scheutjens et al.[5,6] extended Roe's theory (again, for uncharged polymers) to consider the local conformations of segments along the polymer backbone by calculating the size and frequency distributions of loops, trains, and tails on the chain; Figure 1 gives illustrative definitions of these terms. The existence of tails can strongly affect various properties of adsorbed polymer layers, such as hydrodynamic layer thickness, latex stability, and the permeability of porous materials in polymer solutions.[7]

The lattice theories of Roe and of Scheutjens and Fleer for adsorption of uncharged polymers have been extended to describe adsorption of strong polyelectrolytes[8,9] and of weak polyelectrolytes[10,11] by including a description of long-range electrostatic interactions. These models provide a fairly detailed description of polyelectrolyte adsorption and have been widely applied.[12-15] Muthukumar[16] has used a path-integral approach to determine the conditions (i.e., chain charge density, solution ionic strength, temperature) that induce polyelectrolyte adsorption on an ionized surface; no calculations or comparisons with experiment have been presented for this theory.

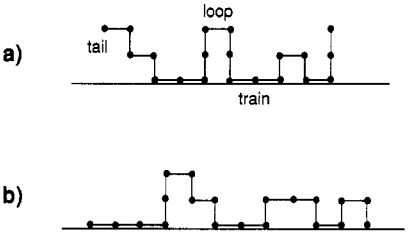

Figure 1. Schematic representation of two potential conformations for a 20-segment adsorbed chain in two dimensions. The chain is represented as a sequence of tails, trains, and loops when adsorbed to a planar surface.

A key question in the study of polyelectrolyte adsorption concerns the structure of the adsorbed species. Polyelectrolytes in solution can have rather well-defined conformations (e.g., collapsed globule; extended rod) and, under certain conditions, can undergo transitions in which major structural rearrangement occurs (e.g., the coil to rod transition).[17] For polyelectrolytes having a specific conformation in solution, a central question addresses how much of that conformation is retained (or lost) upon adsorption.

The detailed interfacial structure of adsorbed polymers and the potential structural changes that occur during adsorption are difficult to investigate experimentally. Monte Carlo simulation can contribute toward such investigations by allowing direct observation of specific molecular configurations for model polyelectrolytes remote from and near interfaces. We have previously used Monte Carlo simulation for studying conformations of isolated polyelectrolytes on an infinite lattice (i.e., remote from an

* To whom correspondence should be addressed.
† Present address: Departamento de Ingeniería Química, Colegio Universitario de Burgos, Universidad de Valladolid, 09002 Burgos, Spain.
‡ Present address: Air Products and Chemicals, Allentown, PA 18195.

0024-9297/91/2224-3178$02.50/0

interface).[18,19] In this work, we use Monte Carlo simulation to examine the conformations of isolated polyelectrolytes in the vicinity of a charged surface. We analyze the changes in conformation that the model polyelectrolytes experience upon adsorption, and we characterize the conformations of the adsorbed chains by the loops, trains, and tails formed at the interface.

Because we consider isolated polyelectrolytes, features resulting from *interchain* interactions will not be observed. Also, we consider only *electrostatic* chain–surface interactions; thus, this work identifies the influence of intrachain and chain–solution interactions on adsorption driven by electrostatic segment–surface attractions. Future work[20] will consider the effect of a nonelectrostatic adsorption energy and the effects of interchain interactions.

II. Simulation Method

A. Model. Our physical model is a single, flexible polyelectrolyte near an impenetrable, uniformly charged surface; Figure 1 shows a two-dimensional representation. We describe here the general features of the model, i.e., when both electrostatic and dispersion-force interactions are possible. In this paper, however, we consider the limiting case in which the nonelectrostatic adsorption energy is zero; i.e., we isolate attention on the effect of electrostatic surface–chain interactions.

The polymer chain in the absence of the surface is identical with the model used in refs 18 and 19 for studying configurational properties of isolated polyelectrolytes. The chain is represented as a self-avoiding walk of N segments on a cubic lattice. The distance between lattice sites, l, is taken as 2.52 Å, which is the distance between alternate atoms on a carbon backbone, assuming tetrahedral geometry and a carbon–carbon bond length of 1.54 Å. Thus, the segments here can be considered analogous to the repeating groups on a vinyl polymer (e.g., poly(acrylic acid)). A fraction, λ, of the segments carry charge of valence unity; these ionized monomers are equally spaced along the chain. All pairs of nonbonded, nearest-neighbor segments interact with potential ϵ. The solvent is considered to be a continuum.

The configurational energy for the isolated chain is given as a sum of electrostatic and nonelectrostatic (dispersion-force) contributions:

$$E = E_{el} + E_{nel} \tag{1}$$

The nonelectrostatic energy is

$$E_{nel} = \epsilon m \tag{2}$$

where m is the total number of contacts between nonbonded, nearest-neighbor segments. The electrostatic energy is the sum over long-range Coulombic interactions between all pairs of ionized segments:

$$E_{el} = \sum_{i}^{N-1} \sum_{j=i+1}^{N} u_{ij} \tag{3}$$

Here u_{ij} is described by a screened Debye–Hückel Coulombic potential[21]

$$u_{ij} = \frac{z_i z_j e^2}{D r_{ij}} \exp(-\kappa r_{ij}) \tag{4}$$

where $z_i e$ and $z_j e$ are the charges on segments i and j that are separated by distance r_{ij}. The ion valence, z, is either 1 or 0; when segment i or j is uncharged, $u_{ij} = 0$. The dielectric constant, D, is taken as that of water at 25 °C. The inverse Debye screening length, κ, is defined by

$$\kappa^2 = \frac{4\pi e^2 N_A \sum_i z_i C_i}{DkT} \tag{5}$$

where N_A is Avogadro's number, C_i is the concentration of ionic species i, k is Boltzmann's constant, and T is the absolute temperature.

In addition, we must consider interaction between the polyelectrolyte and the surface. The energy for the polyelectrolyte–surface interaction is a sum of two contributions:

$$E' = E'_{el} + E'_{nel} \tag{6}$$

In this work, we consider the case where $E'_{nel} = 0$. The polymer–surface electrostatic energy, E'_{el}, is the sum of all Coulombic interactions between the charged polymer segments and the ionized surface sites

$$E'_{el} = \sum_{i=1}^{N} u_{si} \tag{7}$$

where u_{si} depends on the charge on segment i and on the electrostatic potential, Φ, at the position of that segment:

$$u_{si} = z_i e \Phi \tag{8}$$

Gouy and Chapman considered the problem of a charged planar surface in contact with an electrolyte solution. They suggested that the ions which neutralize the surface charge are spread into the solution, forming a diffuse double layer. We assume that, since the polyelectrolyte solution is very dilute (we are studying a single chain in a medium that is infinite in two dimensions), the polyelectrolyte does not contribute to the ionic strength of the solution. We consider an infinite, uniform surface situated in the y–z plane at $x = 0$ and with a homogeneous charge density. The electrostatic potential Φ is a function only of the distance x from the surface; there are no variations of this potential along the y or z coordinates. Thus, we write the Poisson–Boltzmann equation for the variation of the electrostatic potential with distance from the surface in the following form:[22]

$$\frac{d^2\Phi}{dx^2} = \frac{4\pi e}{D} \sum_i z_i n_i \exp\left(\frac{-z_i e \Phi}{kT}\right) \tag{9}$$

where D is the dielectric constant of the medium (water at 25 °C), z_i is either a positive or negative valence number for the ions in solution, and n_i is the concentration of ions of type i in solution.

Equation 10 can be solved by considering only the situation in which $z_i e\Phi < kT$, so that the exponential can be expanded as a power series. Equation 10 then takes a simple form with an explicit solution. Evaluating the potential at 25 °C for a monovalent ion that satisfies the condition $z_i e\Phi = kT$, a potential of 25.7 mV is obtained. Thus, potentials may be regarded as low or high, compared to a potential of (about) 25 mV. Debye and Hückel[22] made the assumption of low potentials in their theory known as the Debye–Hückel approximation.

Gouy and Chapman solved the Poisson–Boltzmann equation without the low-potential assumption for a symmetrical electrolyte solution ($z_i = z$ *and* $n_i = n$ for all the ions in solution) to obtain the variation of the electrostatic potential with distance from the charged surface. By introducing the substitution

$$b = 2kT/ze \tag{10}$$

the expression obtained for the potential is[22]

$$\Phi = b \ln \frac{\exp\left(\frac{\Phi_0}{b}\right) + 1 + \left[\exp\left(\frac{\Phi_0}{b}\right) - 1\right]e^{-\kappa x}}{\exp\left(\frac{\Phi_0}{b}\right) + 1 - \left[\exp\left(\frac{\Phi_0}{b}\right) - 1\right]e^{-\kappa x}} \quad (11)$$

where κ is the inverse Debye screening length as defined in eq 5, x is the coordinate normal to the surface, and Φ_0 is the potential at $x = 0$; that potential is a function of the surface charge density σ[22]:

$$\Phi_0 = b \sinh^{-1}\left[\sigma\left(2\frac{D}{\pi}\kappa \mathrm{T} n\right)^{1/2}\right] \quad (12)$$

Initially we used both the Debye–Hückel[22] and Gouy–Chapman[21] theories for calculating the potential Φ, and the results of the two methods were compared. For surface potentials below approximately 40 mV, the two theories give essentially the same results; however, for higher potentials, significant differences between the two methods were observed. Thus, all calculations reported here were made by using Gouy–Chapman theory.

The total configurational energy of the polyelectrolyte–interface system, E_{tot}, is the sum of the electrostatic polyelectrolyte–surface energy and both electrostatic and nonelectrostatic energies for the segment–segment interactions

$$E_{tot} = E + E'_{el} \quad (13)$$

where E is obtained from eq 1 and E'_{el} from eq 7.

B. Sampling Method. We consider in this work several features of polyelectrolyte adsorption. First, for a polyelectrolyte that can "see" a charged surface, we wish to know how close that polyelectrolyte migrates to the surface (i.e., whether or not it adsorbs and how strongly it does so). Second, for cases where adsorption occurs, we are interested in the interfacial structure of the adsorbed species as described by the local conformation at the surface (see section C below). Finally, we want to examine how the adsorption process affects overall chain dimensions and structure with respect to the dilute chain remote from an interface. Thus, we need to efficiently sample the configurational space of the polyelectrolyte itself (i.e., the internal chain structure) and the configurational space of the overall system (i.e., allowing the polyelectrolyte to migrate close to or remain remote from the surface). We describe below the sampling procedure employed here.

The chain was initially placed in a three-dimensional staircase configuration and then allowed to undergo elementary motions. As in ref 19, two general types of chain movements were used: reptation and "internal" motions. Reptation[23] resembles a "slithering" of the chain along the lattice, resulting in a net forward or backward displacement of all segments; these motions allow the polyelectrolyte to efficiently explore its environment, i.e., either to migrate to or remain remote from the interface. Internal motions involve the rearrangement of one or two internal-chain segments and allow for efficient sampling of high-density conformations (e.g., collapsed or adsorbed conformations). As in ref 19, we use here both reptation and internal motions for sampling; the two types of movements are attempted with equal frequency.

Successive "trial" configurations (generated from elementary chain motions) are accepted based on the probability

$$p_{s+1} = \min\{1, \exp(-\Delta E/kT)\} \quad (14)$$

where ΔE is the energy change in going from configuration s to trial configuration $s + 1$. When a trial move is accepted, configuration $s + 1$ becomes configuration s, and a new move is attempted (i.e., a new trial configuration $s + 1$ is generated). When a trial move is rejected, the old configuration (s) is retained and considered as the new state. In this manner, the polymer *evolves* through a sequence (or chain) of configurations generated by successive cycles (attempted elementary motions).

After relaxing the initial configuration through 5×10^4 cycles, the system was allowed to evolve through 2×10^6 cycles, and chain properties were calculated and recorded every 10^4 cycles. The specific initial conformation used is unimportant since its memory is lost during the relaxation step. All simulations were performed with 40-segment chains; the sampling frequency of 10^4 cycles was found satisfactory for producing essentially uncorrelated configurations for this chain length.

C. Calculated Properties. We describe here the properties used for characterizing chain configuration and position relative to the surface. These properties were calculated every 10^4 cycles during a simulation, and ensemble averages of these properties (denoted by $\langle\ \rangle$) were calculated at the end of a simulation run.

Due to the anisotropic shape of an adsorbed polymer, the three components of the end-to-end distance are not equal. Mean-square end-to-end distance $\langle r^2 \rangle$ and the components of this distance orthogonal ($\langle r^2 \rangle_o$) and parallel to the surface ($\langle r^2 \rangle_p$) were calculated as

$$\langle r^2 \rangle = \langle (\mathbf{r}_n - \mathbf{r}_1)^2 \rangle \quad (15)$$

$$\langle r^2 \rangle_o = \langle (x_n - x_1)^2 \rangle \quad (16)$$

$$\langle r^2 \rangle_p = \langle (y_n - y_1)^2 + (z_n - z_1)^2 \rangle \quad (17)$$

Similarly, it is useful to compute the contributions to the mean-square radius of gyration $\langle s^2 \rangle$ in the planes parallel, $\langle s^2 \rangle_p$, and orthogonal, $\langle s^2 \rangle_o$, to the surface:

$$\langle s^2 \rangle = \frac{1}{N}\left\langle \sum_{i=1}^{N} (\mathbf{r}_i - \mathbf{r}_{cm})^2 \right\rangle \quad (18)$$

$$\langle s^2 \rangle_o = \frac{1}{N}\left\langle \sum_{i=1}^{N} (x_i - x_{cm})^2 \right\rangle \quad (19)$$

$$\langle s^2 \rangle_p = \frac{1}{N}\left\langle \sum_{i=1}^{N} (y_i - y_{cm})^2 + (z_i - z_{cm})^2 \right\rangle \quad (20)$$

Here x_i, y_i, and z_i are the Cartesian coordinates of bead i, $\mathbf{r}_i$ is the position vector locating the ith bead, and subscript cm stands for the center of mass of the chain. The end-to-end distances and radii of gyration are reported in this work as reduced variables. The mean-square end-to-end distance and its components are reduced by the value they would have in a fully extended configuration, $(N-1)^2 l^2$, and the mean-square radius of gyration and its components are reduced by $(N-1)l^2$.

The surface is located in the y–z plane (orthogonal to the x axis) at $x = 0$. Lattice layers are numbered ly = 1, ..., 100. The surface layer is at lattice layer ly = 0. To determine the position of the chain relative to the surface, we calculate the average distance from the surface of the chain center of mass and the segment-density distribution along the coordinate normal to the surface.

To characterize the conformation of the adsorbed polyelectrolyte chain, we consider the content of local conformations known as tails, trains, and loops. Figure 1 shows

(in two dimensions) two potential conformations for a 20-segment chain. Trains are consecutive segments in contact with the surface; loops are consecutive segments between trains, and tails are series of segments at the chain ends which are not in contact with the surface. The number of segments in a loop, train, or tail determines its size; i.e., the chain in Figure 1a consists of 2 tails of sizes 4 and 2, 2 trains of size 3, 1 train of size 2, and 2 loops of sizes 4 and 2. Figure 1b shows a configuration where the ends of the chain are trains of respective sizes 4 and 1; this configuration does not contain tails.

We use here two different types of distributions to present information concerning the loop, train, and tail content in adsorbed chains. In the first type of distribution, we are concerned with how far into the solution (i.e., away from the surface) the different types of elementary structures protrude. Thus, for a given lattice layer parallel to the surface, we count the number of segments in that layer contributing to each of the three structures of interest. Trains are always in layer ly = 1 and thus are not considered in this distribution. For this first distribution, we plot the number frequency of segments contributing to the three types of structures as a function of lattice layer away from the surface. The second type of distribution is concerned with the *size* frequency of the three types of local structures. Here, we plot the relative frequencies of loops, trains, and tails as a function of structure size. The differences between the two distributions is seen more readily in the discussion of results that follows.

III. Results and Discussion

In ref 18 and 19, we investigated the configurational properties of *isolated* polyelectrolytes; ref 18 considered *hydrophilic* polyelectrolytes (segment–segment potential $\epsilon/kT = 0$) and ref 19 considered hydrophobic polyelectrolytes ($\epsilon/kT < 0$). Using refs 18 and 19 as a basis, we consider here the effects of polymer, solution, and surface conditions on the structural properties of hydrophilic and hydrophobic polyelectrolytes *near an adsorbing surface*. We consider a charged surface where the nonelectrostatic segment–surface energy is zero; thus, we isolate the effects of *electrostatic* segment–surface interactions on system behavior.

We investigate system behavior as a function of chain ionization (λ), Debye screening length (κ^{-1}), and surface charge density (σ). All runs were performed for 40-segment chains, and chain ionization varied from $\lambda = 0$ (no charged beads) to $\lambda = 0.5$ (20 charged beads). Four values of κ^{-1} were used corresponding to 1:1 electrolyte concentrations of 1.0 M ($\kappa^{-1} = 3.04$ Å), 0.1 M ($\kappa^{-1} = 9.62$ Å), 0.01 M ($\kappa^{-1} = 30.4$ Å), and 0.001 M ($\kappa^{-1} = 96.2$ Å); the surface charge density varied between 0.0005 and 0.05 e/Å^2.

Figures 2 present the effect of surface charge density (σ) and polyelectrolyte ionization (λ) on the orthogonal, parallel, and total components of the end-to-end distance for the case where there are no segment–segment nonelectrostatic interactions ($\epsilon/kT = 0$), and electrostatic interactions are not highly screened ($\kappa^{-1} = 96.2$ Å). In ref 18, it was found that polyions exhibit a transformation from random-coil to rigid-rod behavior as the degree of chain ionization increases; Figures 2 show that polyelectrolytes near a charged surface experience the same coil-to-rod transformation with increasing chain ionization. Figure 2a shows that the parallel component of the end-to-end distance depends little on the surface charge density; the orthogonal component depends noticeably on surface charge at high chain ionization (where adsorption occurs). The total end-to-end distance (Figure 2b) is not significantly different than that for isolated polyelectrolytes in solution (ref 18).

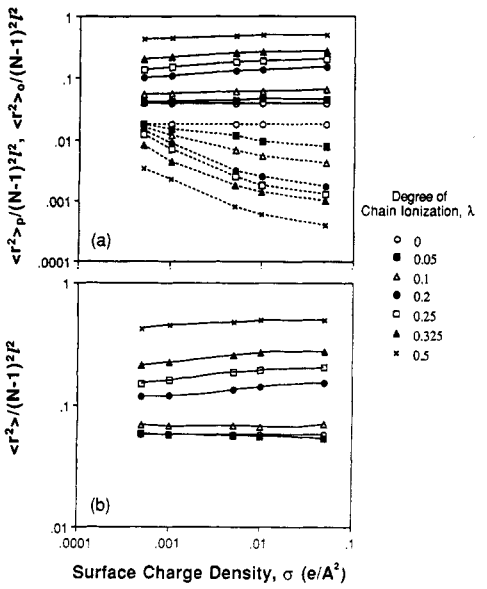

Figure 2. Effect of surface charge density and degree of ionization on polyelectrolyte mean-square end-to-end distance for $\epsilon/kT = 0$ and ionic strength = 0.001 M: (a) parallel (—) and orthogonal (- - -) components; (b) overall (three-dimensional) mean-square end-to-end distance.

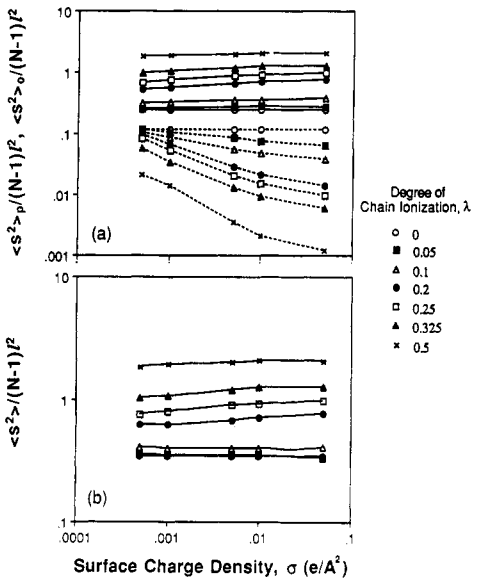

Figure 3. Effect of surface charge density and degree of ionization on polyelectrolyte mean-square radius of gyration for $\epsilon/kT = 0$ and ionic strength = 0.001 M: (a) parallel (—) and orthogonal (- - -) components; (b) overall (three-dimensional) mean-square radius of gyration.

Figure 3 presents the dependence of the mean-square radius of gyration on surface charge density and degree of ionization; the results in Figure 3 are analogous to those seen in Figure 2 for the end-to-end distance.

From Figures 2 and 3, we observe that the overall dimensions and flexibility (or stiffness) of the adsorbed polyelectrolytes are very similar to those of isolated polyelectrolytes in solution at the same conditions. The primary difference is the loss of conformational isotropy for the adsorbed case; as the polyelectrolyte adsorbs, its conformation flattens to decrease the orthogonal components of the end-to-end distance and radius of gyration.

Figure 4 shows the effect of surface charge density and

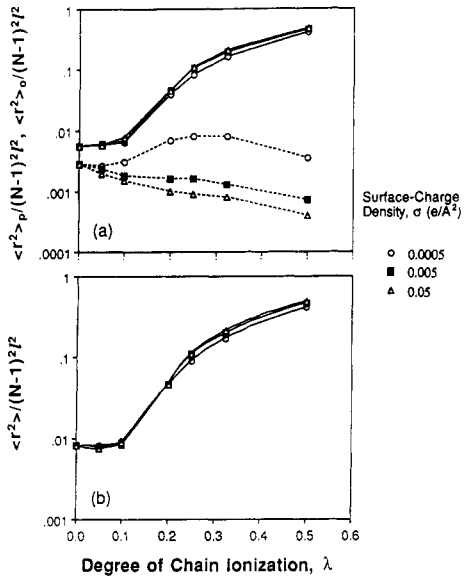

Figure 4. Effect of degree of ionization and surface charge density on polyelectrolyte mean-square end-to-end distance for $\epsilon/kT = -1$ and ionic strength = 0.001 M: (a) parallel (—) and orthogonal (- - -) components; (b) overall (three-dimensional) mean-square end-to-end distance.

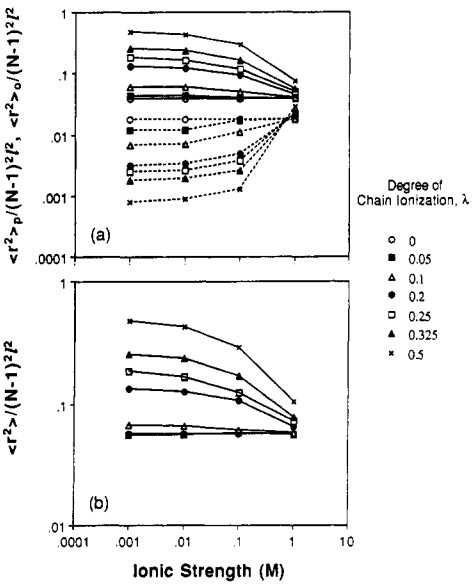

Figure 5. Effect of ionic strength and degree of ionization on polyelectrolyte mean-square end-to-end distance for $\epsilon/kT = 0$ and $\sigma = 0.005$ e/Å²: (a) parallel (—) and orthogonal (- - -) components; (b) overall (three-dimensional) mean-square end-to-end distance.

polyelectrolyte ionization on the orthogonal and parallel components of the mean-square end-to-end distance when polymer segments interact with a pair potential $\epsilon/kT = -1$. Again, the ionic strength is chosen to be sufficiently low (0.001 M) such that electrostatic effects are not highly screened. We plot the parallel and orthogonal components of the end-to-end distance vs degree of ionization to allow comparison of our results with those of ref 19 for isolated hydrophobic polyelectrolytes. Figure 4b shows that, as ionization increases, the overall end-to-end distance of polyelectrolytes near an attractive interface undergoes a transition similar to that seen in ref 19 for isolated polyelectrolytes. However, Figure 4a shows that this transition in chain dimensions is strongly anisotropic; the transition occurs primarily in the parallel component of the end-to-end distance, while the orthogonal component gradually *decreases* with increasing ionization.

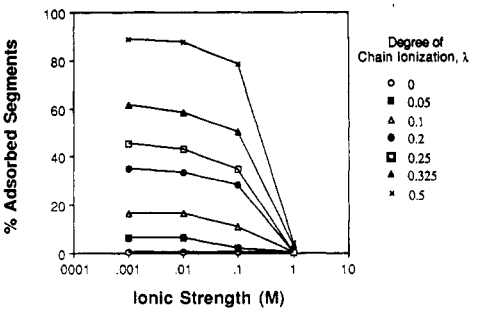

Figure 6. Effect of ionic strength on the percentage of segments adsorbed to the surface for different degrees of chain ionization. Here, the surface charge density $\sigma = 0.005$ e/Å², and the segment–segment nonelectrostatic potential $\epsilon/kT = 0$.

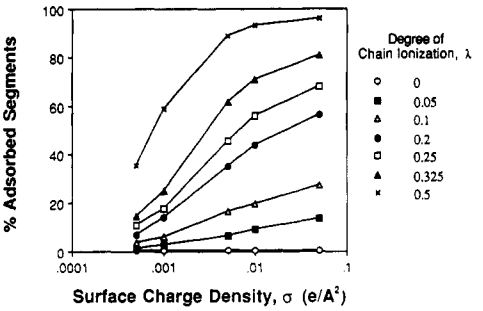

Figure 7. Effect of surface charge density on the percentage of segments adsorbed to the surface for different degrees of chain ionization. Here, ionic strength = 0.001 M and $\epsilon/kT = 0$.

Figures 2–4 consider chain behavior at a constant ionic strength of 0.001 M. Figures 5 and 6 consider the effect of ionic strength on chain end-to-end distance. Here the surface charge density is fixed at $\sigma = 0.005$ e/Å², and nonelectrostatic interactions between polymer segments are set to zero (i.e., $\epsilon/kT = 0$). As ionic strength rises, electrostatic interactions (intrachain and chain–surface) are screened. The reduced Coulombic attraction of the chain to the surface results in an increased orthogonal component of the end-to-end distance (Figure 5a). However, the overall chain dimensions decrease with rising ionic strength (as in the isolated chain case of ref 18) because of the screening of intrachain electrostatic repulsions (Figure 5b). When the ionic strength is 1 M, the chain is essentially desorbed (see Figure 6) and the contributions of the three components to the end-to-end distance converge to the same value; at this point, the parallel component is approximately twice that of the orthogonal component. The influence of ionic strength on chain dimensions is less noticeable for low degrees of ionization.

Summarizing the results of Figure 5, we see that the influence of ionic strength on the *overall* chain dimensions (Figure 5b) of an adsorbed polyelectrolyte is very similar to that for an isolated polyelectrolyte.[18] However, an analysis of the separate end-to-end distance components (Figure 5a) shows a pronounced anisotropic variation, which indicates a transformation in chain *shape*. This change in shape accompanies chain desorption (or adsorption).

Figure 6 shows clearly the chain desorption induced when ionic strength rises. At low ionic strength (0.001 M), the percent of segments that are adsorbed increases from 0 to nearly 90% as chain ionization increases from 0 to 0.5. As ionic strength rises, the number of adsorbed segments falls, until at 1.0 M the chain does not adsorb to the surface for any of the degrees of ionization studied.

Figure 7 shows the variation in the number of adsorbed segments as a function of surface charge density for

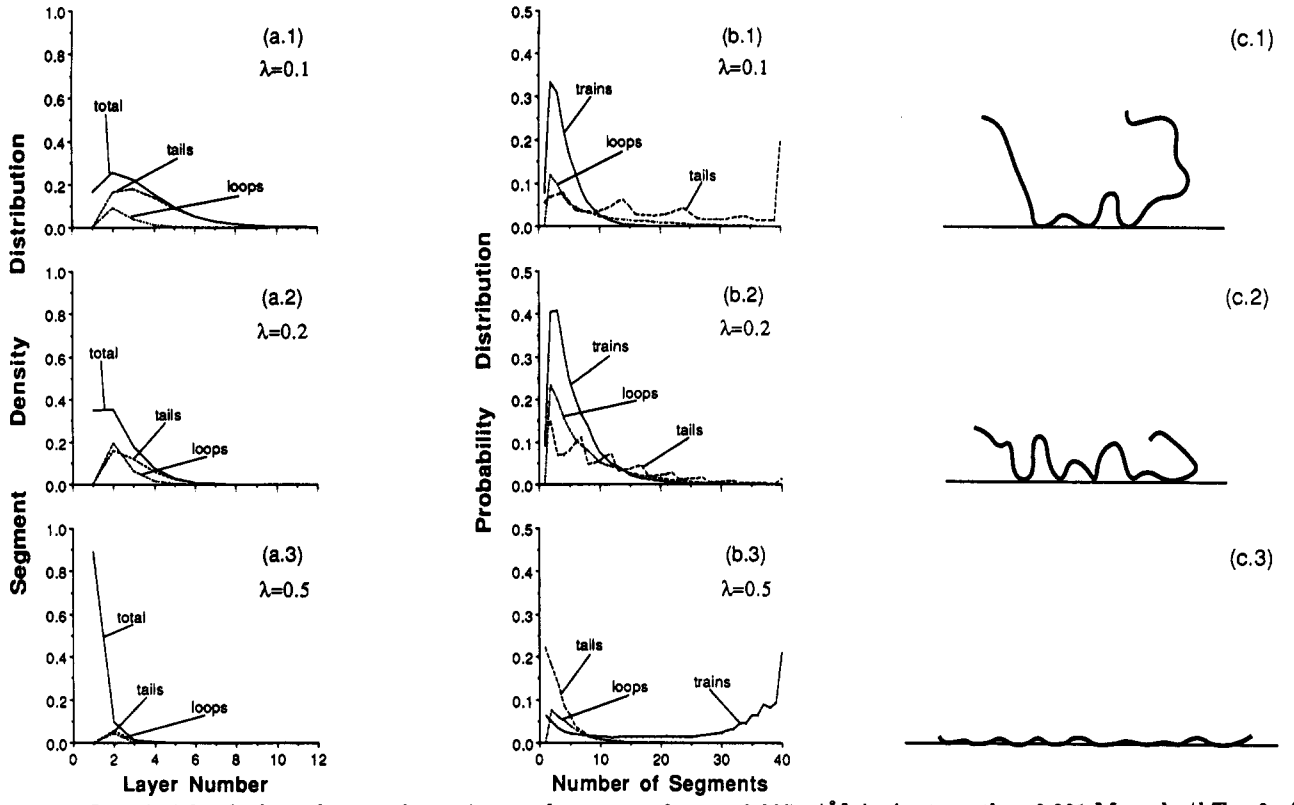

Figure 8. Interfacial polyelectrolyte conformations and structure for $\sigma = 0.005$ e/Å^2, ionic strength = 0.001 M, and $\epsilon/kT = 0$: (a) segment density distribution (—), density distribution of segments contained in loops (· · ·), and density distribution of segments contained in tails (- - -) along the coordinate orthogonal to the surface; (b) size frequency distribution of tails (- - -), trains (—), and loops (· · ·); (c) schematic illustrations of the different conformations adopted by an adsorbed chain as a function of degree of ionization.

different degrees of chain ionization. As the surface charge density increases, the number of adsorbed segments increases; this effect is stronger for higher degrees of chain ionization.

Figure 8 considers the effect of *degree of adsorption* (i.e., how close a chain is held to a surface) on the polymer interfacial structure. Figure 8, parts a and b, presents distributions of segment densities, along with loop, train, and tail content, for chains that are qualitatively analogous to those shown in the corresponding column of Figure 8c. Figure 8a shows the segment-density distribution along the coordinate perpendicular to the surface and the density distribution of segments that are part of a loop or a tail for the following conditions: surface charge density σ = 0.005 e/Å^2, ionic strength IS = 0.001 M, and pair potential interaction between polymer segments $\epsilon/kT = 0$. Figure 8b shows the distribution of tails, trains, and loops by size for the same conditions. The degree of chain ionization varies; $\lambda = 0.1$ in Figure 8(a,b).1; $\lambda = 0.2$ in Figure 8(a,b).2, and $\lambda = 0.5$ in Figure 8(a,b).3.

The three graphs in Figure 8a show that the segment-density distribution narrows as the degree of ionization increases and the chain adsorbs more strongly. For λ = 0.5, the chain remains primarily in the three lattice layers closest to the surface, and nearly 90% of the segments are adsorbed; the number of adsorbed segments (segments in lattice layer ly = 1) increases with the degree of ionization. Figure 8a.1 shows that, for $\lambda = 0.1$, the segment-density distribution is mostly composed of tails, and these tails extend as far as 15 lattice layers away from the surface; loops are a relatively minor contribution in this case. The contribution of tails to the total segment density distribution decreases as the degree of ionization increases and as the number of segments forming trains undergoes a corresponding increase. Thus, we see that, for low degrees of chain ionization, tails extend further from the surface than loops, and these tails comprise the main contribution to the thickness of the adsorbed layer. However, as chain ionization rises (and adsorption increases), the contributions of tails and loops to the adsorption layer become approximately equal.

Figure 8b shows that for a degree of ionization of λ = 0.1 (Figure 8b.1) there is a large number of 40-segment tails. Since we are studying a 40-segment chain, a 40-segment tail indicates that none of the segments of the chain are adsorbed (free chain). However, we saw in Figure 8a.1 that the chain is attracted to the surface at these conditions. Long tails are favored at low degrees of ionization, while short tails become more favorable as the degree of ionization (and adsorption) increases; for λ = 0.5, long tails are rare. The segment that ends a tail (i.e., the first adsorbed segment starting from either end of the chain) is more likely to be an ionized segment than one that is uncharged. This is seen in Figure 8b by small maxima for such tail sizes; i.e., in Figure 8b.1, the distribution for a 10% ionized chain (where the charged segments are positioned in segments 5, 15, 25, and 35) has maxima for tails that are 4, 14, 24, and 34 segments long respectively. Trains are scarce and short for a 10% ionized chain. As the chain degree of ionization increases, the number of small trains initially rises and then falls while the number of long trains increases.

Figure 8 considers the case of a hydrophilic polyelectrolyte. For a hydrophobic polyelectrolyte, the distributions of segments, tails, trains, and loops show a large number of small trains and loops when the chain ionization is low so that the chain is collapsed, and loops and tails do not protrude as far into the solution as for the hydrophilic polyelectrolyte. When the degree of chain ionization is high enough to adopt a more stretched configuration, all the distributions are similar to those for the hydrophilic polyelectrolyte.

IV. Conclusions

We have studied the behavior of an isolated, partially ionized polyelectrolyte near an impenetrable, oppositely charged surface using Monte Carlo simulation. Configurational properties for the polyelectrolyte near the attractive interface were compared with those for an isolated polyelectrolyte. Differences for the overall end-to-end distance and radius of gyration between the two cases were small. However, large anisotropy was seen between the various components of the chain dimensions when the polyelectrolyte is close to (or adsorbed on) the surface.

The solution ionic strength influences both chain configurational properties and the tendency of the chain to adsorb. At low ionic strength, charge screening is negligible and electrostatic attractions between the surface and chain cause the polyelectrolyte to flatten out and adsorb on the surface. As ionic strength increases, both surface–chain attractions and segment–segment repulsions are screened; thus, the chain assumes a flexible-coil configuration and does not adsorb to the surface.

The detailed interfacial properties of adsorbed chains were studied by considering the distributions of elemental structures such as tails, trains, and loops. At low degrees of chain ionization, the polyelectrolytes adsorb through attachment of only a few segments to the surface, and long tails extend into solution. At high degrees of ionization, many segments adsorb to the surface, and long trains are favored. The number of adsorbed chain segments also increases with rising surface charge density, and decreases with rising ionic strength of the solution.

The conclusions of this work are specific to the case of *isolated* polyelectrolytes at a surface *without* a nonelectrostatic adsorption energy. Direct comparison with experiment is, thus, difficult because real systems are never this simple. However, by considering a idealized problem, this study isolates and identifies the effects of electrostatic segment–surface interactions on adsorption and also provides a basis for future work directed at more realistic systems.[20]

Acknowledgment. This work was supported by the Director, Office of Energy Research, Office of Basic Energy Sciences, Chemical Sciences Division of the U.S. Department of Energy under Contract No. DE-AC03-76SF00098. S.B. is grateful to the Spanish Ministry of Education and Science (MEC) for a fellowship. The calculations reported here were performed on the IBM 3090 at the U.C. Berkeley Computing Center; we acknowledge with thanks the generous computation time provided by the Computing Center. We are grateful to Kevin Mansfield and Doros Theodorou for helpful comments.

References and Notes

(1) Hesselink, F. Th. *J. Electroanal. Chem. Interfacial Electrochem.* **1972**, *37*, 317.
(2) Hesselink, F. Th. *J. Colloid Interface Sci.* **1977**, *60*, 448.
(3) Hoeve, C. A. J. *J. Polym. Sci. C* **1971**, *34*, 1.
(4) Roe, R. J. *J. Chem. Phys.* **1974**, *60*, 4192.
(5) Scheutjens, J. M. H. M.; Fleer, G. J. *J. Phys. Chem.* **1979**, *83*, 1619.
(6) Scheutjens, J. M. H. M.; Fleer, G. J. *J. Phys. Chem.* **1980**, *84*, 178.
(7) Scheutjens, J. M. H. M.; Fleer, G. J.; Cohen Stuart, M. A. *Colloids Surf.* **1986**, *21*, 285.
(8) Van der Schee, H. A.; Lyklema, J. *J. Phys. Chem.* **1984**, *88*, 6661.
(9) Papenhuijzen, J.; Van der Schee, H. A.; Fleer, G. J. *J. Colloid Interface Sci.* **1985**, *104*, 540.
(10) Evers, O. A.; Fleer, G. J.; Scheutjens, J. M. H. M.; Lyklema, J. *J. Colloid Interface Sci.* **1986**, *111*, 446.
(11) Böhmer, M. R.; Evers, O. A.; Scheutjens, J. M. H. M. *Macromolecules* **1990**, *23*, 2288.
(12) Marra, J.; Van der Schee, H. A.; Fleer, G. J.; Lyklema, J. In *Adsorption from Solution*; Ottewill, R. H., Rochester, C. H., Smith, A. L., Eds.; Academic Press: New York/London, 1983; p 245.
(13) Papenhuijzen, J.; Fleer, G. J.; Bijterbosch, B. H. *J. Colloid Interface Sci.* **1985**, *104*, 553.
(14) Cohen Stuart, M. A. *J. Phys. Fr.* **1988**, *49*, 1001.
(15) Blaakmeer, J.; Böhmer, M. R.; Cohen Stuart, M. A.; Fleer, G. J. *Macromolecules* **1990**, *23*, 2301.
(16) Muthukumar, M. *J. Chem. Phys.* **1987**, *86*, 7230.
(17) Oosawa, F. *Polyelectrolytes*; Marcel Dekker: New York, 1971.
(18) Hooper, H. H.; Blanch, H. W.; Prausnitz, J. M. *Macromolecules* **1990**, *23*, 4820.
(19) Hooper, H. H.; Beltran, S.; Sassi, A. P.; Blanch, H. W.; Prausnitz, J. M. *J. Chem. Phys.* **1990**, *93*, 2715.
(20) Sassi, A. P.; Blanch, H. W.; Prausnitz, J. M. Work in progress.
(21) Rieger, P. H. *Electrochemistry*; Prentice Hall: New York, 1987; Chapter 2.
(22) Hiemenz, P. C. *Principles of Colloid Surface Chemistry*, 2nd ed.; Marcel Dekker: New York, 1986; Chapter 12.
(23) Wall, F. T.; Mandel, F. *J. Chem. Phys.* **1975**, *63*, 4592.